



# Stimulus-Responsive Polyelectrolyte Surfaces: Switching Surface Properties from Polycationic/Antimicrobial to Polyzwitterionic/Protein-Repellent

Stefan Paschke, Richard Prediger, Valentine Lavaux, Alice Eickenscheidt, and Karen Lienkamp\*

Surfaces coated with polyzwitterions are most well-known for their ability to resist protein adsorption. In this article, a surface-attached hydrophobically modified poly(carboxybetaine) is presented. When protonated by changes of the pH of the surrounding medium, this protein-repellent polyzwitterion switches to a polycationic state in which it is antimicrobially active and protein-adhesive. The pH range in which these two states exist are recorded by zeta potential measurements. Adsorption studies at different pH values (monitored by surface plasmon resonance spectroscopy) confirm that the adhesion of protein is pH dependent and reversible, that is, protein can be released upon a pH change from pH 3 to pH 7.4. At physiological pH, the poly(carboxyzwitterion) is antimicrobially active, presumably because it becomes protonated by bacterial metabolites during the antimicrobial activity assay. Stability studies confirm that the here presented material is storage-stable, yet hydrolyses after longer incubation in aqueous media.

can help to slow down or shut down the spreading of resistant bacteria, and the develop of biofilms on medical devices. According to a study from 2014, there will be 10 million deaths annually worldwide by 2050 due to bacterial resistance.<sup>[2]</sup> The current pandemic caused by the coronavirus SARS-CoV-2 should give us an idea of how dramatic these numbers are: since the start of the pandemic in 2019 up to today (Jan. 15th, 2021), 2 million lives were lost worldwide. What we are facing by 2050 if current prognoses become reality are five times as many deaths per year due to resistant bacteria, making them a 5 times bigger killer than COVID, and surpassing even the death toll due to cancer. Still, the public is not paying much attention to this threat, even though it is regularly communicated by scientists.


## 1. Introduction

With an unbroken trend towards increasing bacterial resistance against antibiotics,<sup>[1]</sup> there is a pressing need for materials that

Meanwhile, research for novel antibacterial materials is ongoing. A lot of scientific studies have been dedicated to various quite efficient strategies to coat surfaces with antimicrobial and anti-biofilm polymers,<sup>[3–9]</sup> yet only few of these materials made it out of the laboratory and into applications. In many cases, the reason for this is stability problems, that is, the materials are not able to sustain their function under the conditions of application. Thus, while structure–property relationships for such materials are important and have been carried out with great vehemence, now is the time to make sure that these structures also function sufficiently out in the field.

S. Paschke, R. Prediger, V. Lavaux, Dr. A. Eickenscheidt, Prof. K. Lienkamp  
Department of Microsystems Engineering (IMTEK)  
University of Freiburg  
Georges-Köhler-Allee 103, 79110 Freiburg, Germany  
E-mail: karen.lienkamp@uni-saarland.de

S. Paschke, R. Prediger, V. Lavaux, Dr. A. Eickenscheidt, Prof. K. Lienkamp  
Freiburg Center for Interactive Materials and Bioinspired Technologies (FIT)  
University of Freiburg  
Georges-Köhler-Allee 105, 79110 Freiburg, Germany  
Prof. K. Lienkamp  
Institut für Materialwissenschaft und Werkstoffkunde  
Universität des Saarlandes  
Campus, 66123 Saarbrücken, Germany

 The ORCID identification number(s) for the author(s) of this article can be found under <https://doi.org/10.1002/marc.202100051>

© 2021 The Authors. Macromolecular Rapid Communications published by Wiley-VCH GmbH. This is an open access article under the terms of the Creative Commons Attribution-NonCommercial-NoDerivs License, which permits use and distribution in any medium, provided the original work is properly cited, the use is non-commercial and no modifications or adaptations are made.

Until very recently, the accepted paradigm was that contact-active antimicrobial polymer surfaces need to be polycationic, and that polyzwitterionic polymers are protein-repellent but not intrinsically antimicrobial.<sup>[10–16]</sup> We recently demonstrated that this is not a universally valid paradigm using different polyzwitterionic surface-attached polymer networks.<sup>[8,9,17]</sup> These contained mostly weak electrolytes as functional groups. In particular, polyzwitterions with carboxylate groups like **PZI**, **IA-PZI**, and **PCB** (Figure 1) apparently have *pK* values that allow their protonation by surrounding bacteria. Thus, it has been hypothesized that these polyzwitterionic surfaces become polycationic in the presence of bacteria (who secrete acidic metabolites), but remain protein-repellent in their absence. This would make such surfaces switchable and thus potentially resistant against biofilm formation for a longer time than cationic polyelectrolytes containing

DOI: 10.1002/marc.202100051

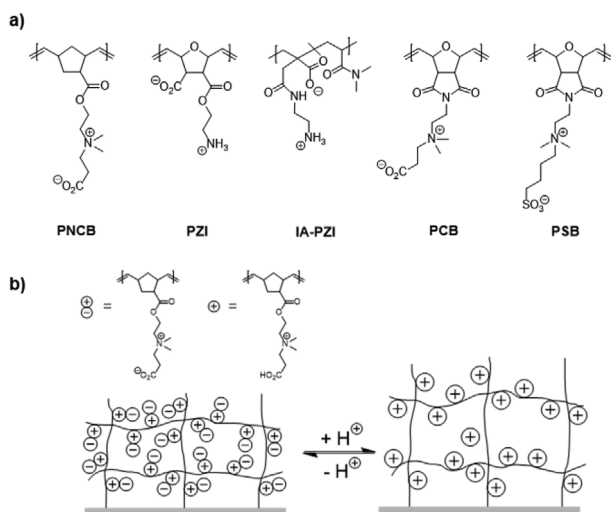


**Figure 1.** Structures of **PNCB** and other antimicrobial polyzwitterions described in the literature. **PZI**,<sup>[8]</sup> **IA-PZI**,<sup>[17]</sup> and **PCB**<sup>[9,18]</sup> are intrinsically antimicrobial when protonated. **PSB**<sup>[8,18]</sup> (used as a reference in this study) is protein-repellent but not active against bacteria. When designing **PNCB**, the imide-ring of **PCB** was replaced by an ester-linker, the backbone was based on norbornene instead of oxanorbornene, and the structure contains a more stable quaternary ammonium group instead of a primary one.

only strong electrolyte groups, since these are permanently adhesive for bacteria and other negatively charged biomolecules.

In this paper, we present the design and synthesis of polymers based on the polyzwitterion **PNCB** carrying a weak and a strong electrolyte group on each repeat unit (Figure 1a). We further report the synthesis and physical surface characterization, the biological properties and stability studies of surface-attached polyzwitterionic networks derived from **PNCB**. The **PNCB** repeat unit was designed for improved stability over its predecessors **PZI** and **IA-PZI** (Figure 1a, who suffer from antimicrobial activity loss related to side reactions that involve their primary amine groups), and over **PCB** (ibid.), which undergoes ring-opening at neutral to basic pH when in contact with aqueous media for more than 24 h. We also present a protein adhesion study that demonstrates the switchability of **PNCB** properties between the protein repellent and the protein adhesive state, that is, the reversible, pH-dependent protein adsorption on and desorption from **PNCB**-based polymers.

## 2. Results and Discussion

### 2.1. Study Design

The aim of the work was to design and study stimulus-responsive, surface-attached polyzwitterionic networks whose surface charge could be switched from polyzwitterionic/protein-repellent to polycationic/antimicrobial, and which did not have the structural drawbacks (labile primary amine groups and imide rings) of previously reported charge-switchable polycationic/polyzwitterionic materials. This should overcome the limited stability from which these materials previously reported by us suffer.<sup>[8,9,17]</sup> The target structures were polymers with **PNCB** repeat units (Figure 1). Three polymers were synthesized: the

homopolymer (**PNCB-Homo**) and two copolymers consisting of **PNCB** repeat units as the major component, and a minor component that carried UV active cross-linker groups. These were either benzophenone or diazo groups, respectively (Figure 2), and were needed to cross-link the target polymer to form a surface-attached polymer network. The polymerization platform chosen was ring-opening metathesis polymerization (ROMP) due to its high functional group tolerance. The functional monomer (**NCB**, Figure 2) was a norbornene derivative instead of the more labile oxanorbornene used in previous work. Its zwitterionic side-chain consisted of a pH-inert quaternary ammonium group and a carboxylate group which was pH responsive. This zwitterion pair was linked to the backbone with an ester group (Figure 2). The cross-linker monomer was an oxanorbornene imide with either a benzophenone group (**PNCB-co-BP**) or a diazo ester (**PNCB-co-Diazo**) in the side chain (Figure 2). In the case of the homopolymer (**PNCB-Homo**), a UV-responsive low molecular mass cross-linker was added to enable network formation.

Each polymer was surface attached to a pre-functionalized silicon substrate by UV irradiation, and then characterized by FTIR spectroscopy, ellipsometry, water contact-angle measurements, and X-ray photoelectron spectroscopy (XPS). To assess the stimulus-responsiveness of the network, its pH-dependent surface zeta potential was determined by electrokinetic measurements. Its pH-dependent adhesiveness for the protein pepsin was studied by surface plasmon resonance spectroscopy (SPR). This was complemented by antimicrobial activity and cell compatibility assays. Additional stability assays were performed under application and storage conditions.

### 2.2. Synthesis, Polymer Characterization, and Polymer Network Fabrication

The monomer **NCB** was synthesized as described in Figure 2a. First, 5-norbornene-2-carboxylic acid **1** was esterified with 2-(dimethylamino)ethanol in a Mitsunobu-type reaction. The reaction product **2** carried a tertiary amine group, by which  $\beta$ -propiolactone was ring-opened in the second step. This gave the desired zwitterionic monomer **NCB** (Figure 2a). Prior to polymerization, **NCB** was protonated by HCl treatment. The **PNCB** homopolymer (**PNCB-Homo**) was synthesized via ROMP using Grubbs 3<sup>rd</sup> Generation catalyst in a mixture of 2,2,2-trifluoroethanol (TFE) and dichloromethane (DCM) (Figure 2b). The cross-linker monomers **3** and **4** needed for the **PNCB** copolymers were synthesized after literature procedures.<sup>[19]</sup> Copolymerization of 90 mol% **NCB** and 10 mol% of monomer **3** gave the copolymer **PNCB-co-BP** which contained 90% functional units and 10% repeat units with a benzophenone cross-linker (Figure 2c). Copolymerization of 90 mol% **NCB** and 10 mol% of **4** resulted in the analogous copolymer **PNCB-co-Diazo** (Figure 2c).

The characterization data of **2**, **NCB** and the polymers obtained by NMR-spectroscopy and FTIR spectroscopy is shown in Figures S1–S13, Supporting Information. Gel-permeation-chromatography (GPC) analytics of the polymers in trifluoroethanol (TFE) is shown in Table 1 (Figure S14, Supporting Information).

The PDI values of the thus obtained **PNCB**-based polymers were rather high for ROMP, but this can be attributed to the

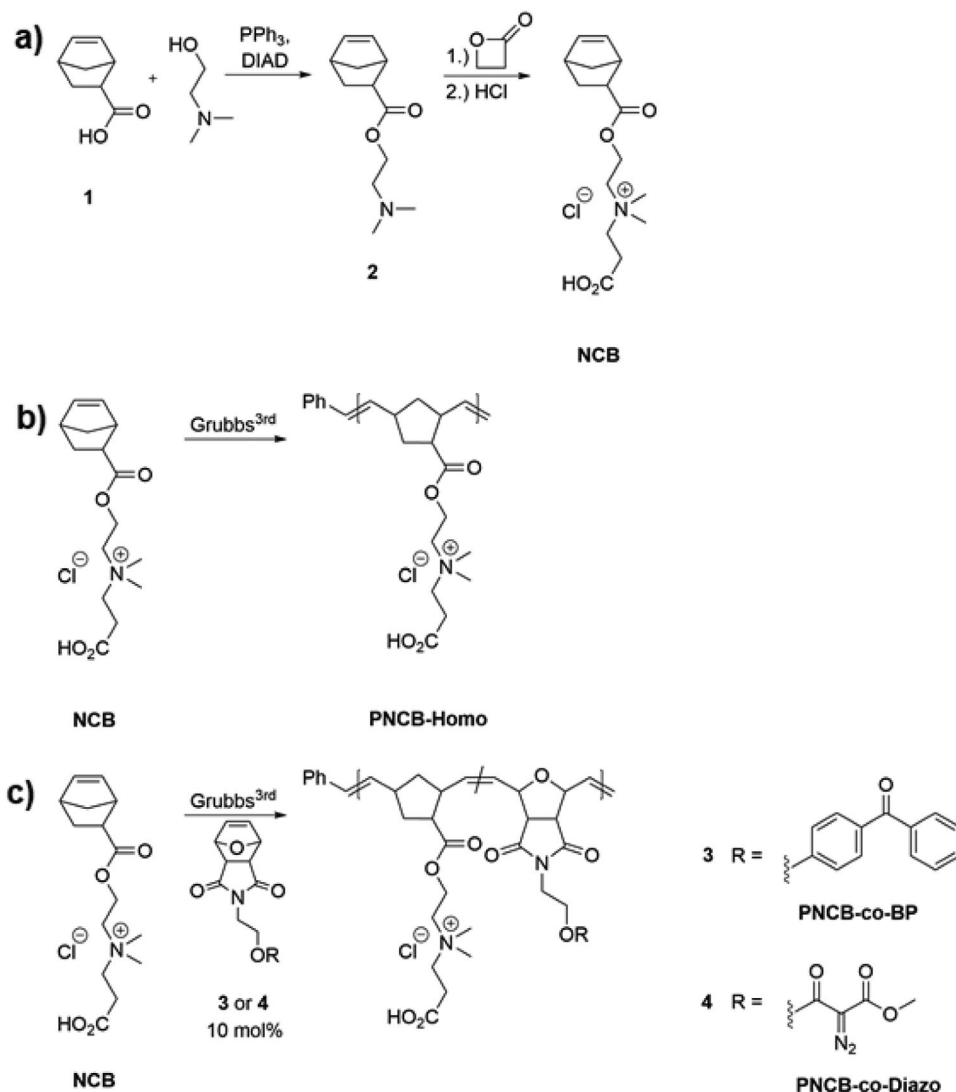


**Figure 2.** a) Synthesis and copolymerization of the monomer **NCB**: Esterification of acid **1** under Mitsunobu conditions (DIAD = diisopropyl azodicarboxylate,  $\text{PPh}_3$  = triphenylphosphane) gave the product **2** with a tertiary amine group. Ring-opening of the lactone and acid treatment yielded the cationic monomer **NCB**; b) homopolymerization of **NCB** via ring-opening metathesis polymerization (ROMP) using Grubbs 3rd generation catalyst yielded **PNCB-Homo**. c) Copolymerization of **NCB** with the crosslinker monomer **3** or **4**, respectively, yielded **PNCB-co-BP** and **PNCB-co-Diazo**.

**Table 1.** Molecular mass of the different **PNCB** copolymers determined by gel permeation chromatography (in TFE, with 0.05 M  $\text{CF}_3\text{CO}_2\text{K}$ , PMMA-standard, PFG-column, 40 °C).

Polymer	$M_n/\text{g mol}^{-1}$	PDI
<b>PNCB-Homo</b>	49 500	1.36
<b>PNCB-co-Diazo</b>	31 700	1.55
<b>PNCB-co-BP</b>	55 900	1.36

use of TFE as a polymerization co-solvent. TFE was needed to solubilize the **NCB** monomer, yet the Grubbs catalyst has only limited stability in this solvent.<sup>[20]</sup> However, since the polymers were used for the fabrication of a surface-coating, a precise molecular weight or a low PDI were not critical. Silicon wafers

were used as model substrates. These had been previously functionalized with a mixture of amine groups and benzophenone groups using (3-aminopropyl)triethoxysilane (**APTES**) and 4-(3-triethoxysilyl)propoxy-benzophenone (**3EBP**) as described in the literature.<sup>[17,21]</sup> Solutions containing the polymers **PNCB-co-BP** or **PNCB-co-Diazo** were spin-coated onto the thus obtained functionalized wafers, which were more hydrophilic than wafers with a pure **3EBP** layer, thus surface dewetting during drying was prevented.<sup>[21]</sup> In the case of **PNCB-Homo**, the tetrafunctional molecule pentaerythritol-tetrakis-(3-mercaptopropionat) was added to the polymer solution prior to spin coating. In each case, the polymer-coated surfaces were then UV irradiated at a wavelength of 254 nm to simultaneously cross-link and surface-attach them. For **PNCB-co-BP**, these conditions activated the benzophenone units both in the **3EBP** linker connected to the surface, and those in the polymer side chains, which then

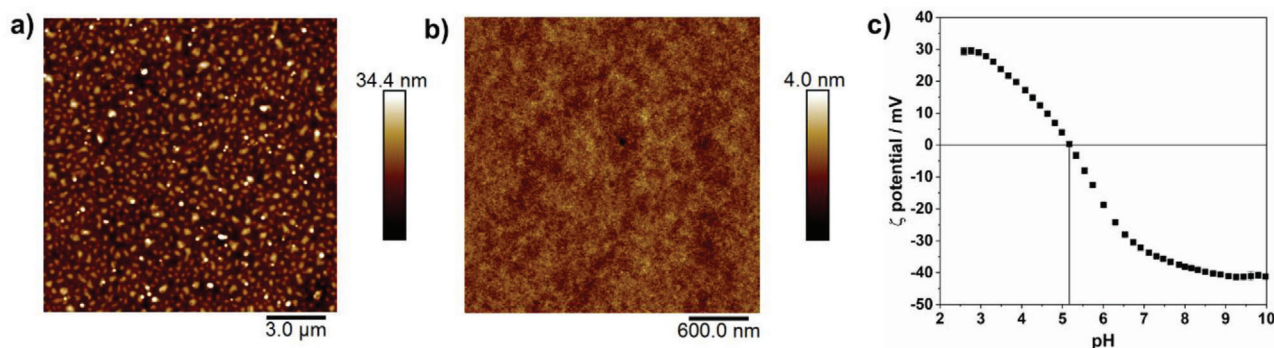


**Figure 3.** a) Representative AFM height image of a surface-attached network from **PNCB-Homo**, with a granular morphology and a rms roughness of  $R_q = 5.0$  nm. b) Representative AFM height image of a surface-attached network from **PNCB-co-BP** with a very smooth surface with a rms roughness of  $R_q = 0.3$  nm. c) pH-dependent surface zeta potential of **PNCB-co-BP** networks obtained by electrokinetic measurements.

underwent C,H-insertion (CHiC) reactions with nearby C–H bonds<sup>[22]</sup> to form a highly cross-linked surface-attached polymer network. For **PNCB-co-Diazo**, a similar process took place after activation of the diazo ester.<sup>[23]</sup> When UV irradiating **PNCB-Homo** and pentaerythritol-tetrakis-(3-mercaptopropionat), a thiol-ene-reaction caused the network formation, while a CHiC reaction with the **3EBP** groups ensured the surface attachment.

The cross-linking efficiency of each network type was determined by measuring the gel content of the network, that is, the fraction of covalently bound polymer chains compared to unbound, extractable polymer chains. For this, the network was extracted with a good solvent for the **PNCB** repeat unit (e.g., trifluoroethanol), and the layer thickness before and after extraction was determined by ellipsometry. The gel content was obtained as the ratio of the polymer layer thickness after extraction divided by layer thickness before extraction, multiplied by 100. The gel contents thus obtained at various irradiation conditions is shown in Figure S15, Supporting Information. The data shows that the gel content of **PNCB-Homo** and **PNCB-co-Diazo** did not exceed 40%. For **PNCB-co-BP**, it was between 65% and 70% in all cases, even at low energy-doses of only  $0.5 \text{ J cm}^{-2}$ . It did not increase with higher irradiation doses, possibly because of the high number of heteroatoms in the repeat units, as discussed in reference.<sup>[19]</sup>

### 2.3. Physical Characterization of PNCB Networks

The surface-attached networks obtained from **PNCB-Homo** and **PNCB-co-BP** were analyzed by atomic force microscopy (AFM) to determine if the substrates were homogeneously covered by the polymer. Homogeneous surface coverage is important to ensure reliable and reproducible data in further investigations. As can be seen in **Figure 3a**, networks formed from **PNCB-Homo** and the additional low molecular mass cross-linker had a granular morphology and a high rms roughness of 5.0 nm. This hints at microphase separation during the coating process. In contrast, a representative AFM height image of **PNCB-co-BP** (**Figure 3b**) demonstrates that a very smooth surface with hardly any features and a rms roughness ( $R_q$ ) of only 0.3 nm were obtained. This result is in good agreement with the literature, where polyzwitterionic networks prepared with a built-in ben-

**Table 2.** pH dependency of the zeta potential of **PNCB-co-BP** and **PCB**; data obtained from electrokinetic measurements. IEP = Isoelectric Point ( $\zeta = 0$  mV),  $\zeta_{\text{phys}} = \zeta$  at pH 7.4. **PCB** data from ref. [9].

Polymer	IEP	$\zeta_{\text{phys}}/\text{mV}$	pK	$\zeta_{\text{max}}/\text{mV}$	$\zeta_{\text{min}}/\text{mV}$
<b>PNCB-co-BP</b>	$5.2 \pm 0.1$	$-35 \pm 5$	$4.1 \pm 0.2$	$30 \pm 5$	$-41 \pm 5$
<b>PCB</b>	$5.4 \pm 0.1$	$-28 \pm 5$	$3.0 \pm 0.2$ $6.5 \pm 0.2$	$50 \pm 7$	n.d.

zophenone cross-linker also were very smooth,<sup>[6,7,24]</sup> in contrast to networks formed from polyzwitterionic homopolymers and additional low molecular mass cross-linkers, which also tended to be granular.<sup>[8,25]</sup>

The pH-dependent surface zeta potential of **PNCB-co-BP** networks was measured via electrokinetic measurements (**Figure 3c** and **Table 2**). In line with the expectations for a pH-responsive polyzwitterion, the zeta potential had a characteristic sigmoidal shape. It was positive at low pH ( $\zeta_{\text{max}} = 30$  mV) and negative at high pH ( $\zeta_{\text{min}} = -41$  mV), with an isoelectric point (IEP) at pH 5.2. This is in good agreement with the data presented in the literature for the surface-attached poly(carboxybetaine) **PCB** (**Figure 1**), which had an IEP at 5.4 and a  $\zeta_{\text{max}}$  of 50 mV.<sup>[9]</sup> At physiological pH, the zeta-potential  $\zeta_{\text{phys}}$  of the network surface was slightly negative, which is also in agreement with literature data ( $\zeta_{\text{phys}}$  of **PCB** =  $-28$  mV). The pK of the carboxylic acid group of **PNCB-co-BP** (determined as previously reported by Kurowska et al.<sup>[9]</sup>) was 4.1. It is thus found at a slightly higher pH value than the value presented in the literature for **PCB**, but it is in the same range as the pK of other carboxylic acids, for example acetic acid with a pK of 4.76. Notably, in contrast to **PZI** (with two pH responsive groups) and **PCB** (which in addition to the pH-dependent carboxylate group ring-opens at a pH >7), **PNCB-co-BP** only has one pH responsive unit, thus its acid-base equilibrium is not affected by the pH dependency of a second such equilibrium. This might explain the differences observed in comparison to **PCB** and **PZI**.

The hydrophilicity of the **PNCB-co-BP** network was confirmed via water contact-angle measurements. The static, advancing and receding contact angles were  $22^\circ \pm 2^\circ$ ,  $21^\circ \pm 1^\circ$ , and  $23^\circ \pm 4^\circ$ , respectively. Thus, the material is very hydrophilic even

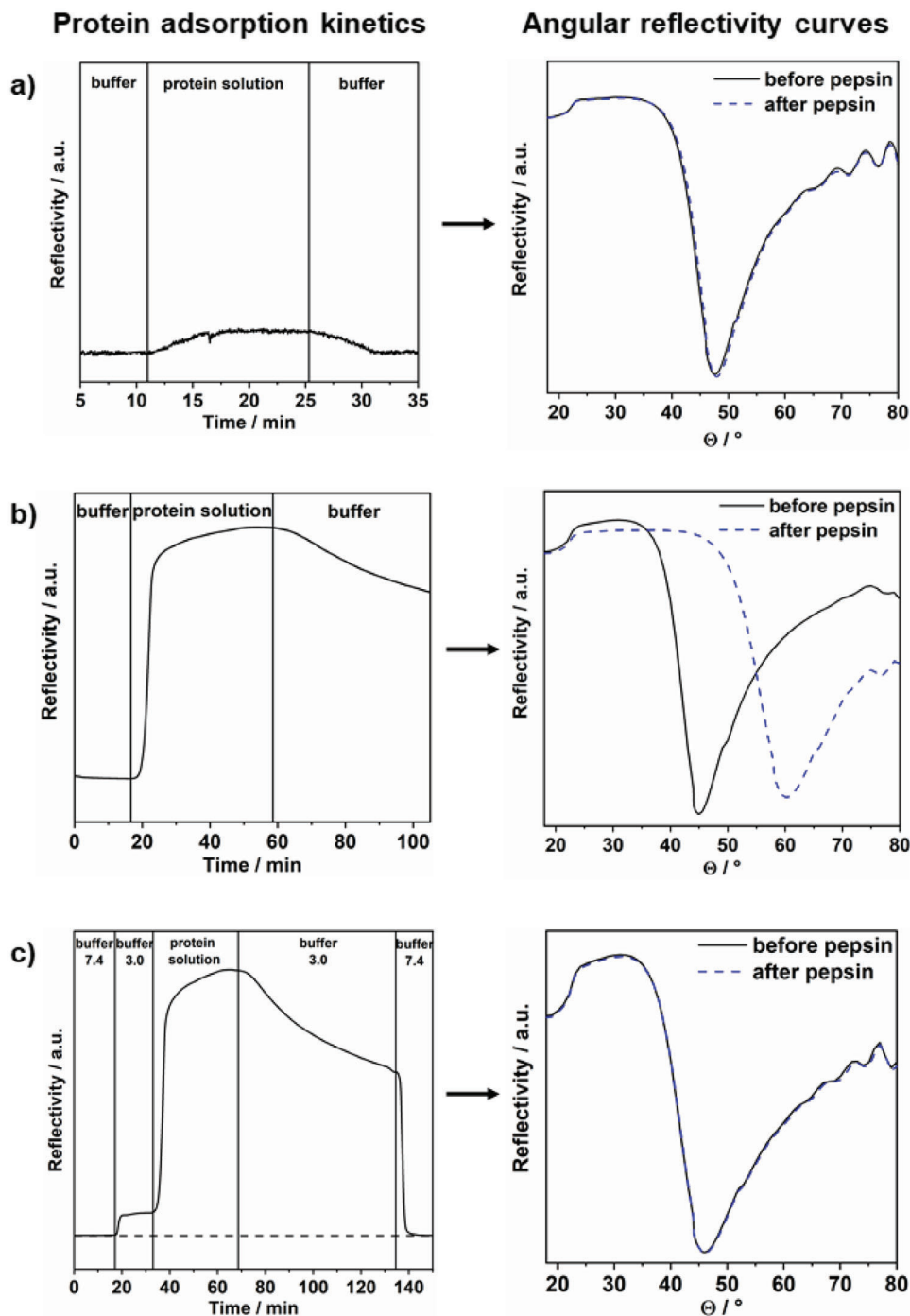


**Figure 4.** Pepsin adhesion on PNCB-co-BP networks studied by surface plasmon resonance spectroscopy. In-situ kinetics measurements and full reflectivity scans (dry substrate before and after contact to pepsin) at a) pH 7.4, and b) pH 3.0 are shown. c) In-situ kinetics measurements demonstrate that a pH change from pH 3.0 to pH 7.4 results in >99% pepsin desorption. This is confirmed by the corresponding full reflectivity scans.

though it contains a hydrophobic backbone and a relatively high amount of repeat units carrying the hydrophobic benzophenone cross linker. Additionally, virtually no contact angle hysteresis was observed. The contact angle data is in the same range as the values reported for other polyzwitterionic networks in the literature.<sup>[9,24,26]</sup>

#### 2.4. Protein Adsorption on Surface-Attached PNCB Networks at Different pH Values

The zeta-potential data showed that the PNCB-co-BP networks were responsive to pH changes, and in consequence could switch from overall positively charged to charge neutral, and even to

**Table 3.** Adsorption of pepsin on **PNCB-co-BP** networks at different pH-values.

pH	Layer thickness of adsorbed pepsin [nm]
3.0	31.3 ± 1
7.4	0.6 ± 1
3.0 → 7.4	0.2 ± 1

negative surface charges at high pH values due to preferential adsorption of anions to the interface. To assess if this property can be used to selectively adsorb and release proteins, a set of adsorption experiments were performed and monitored in-situ by SPR. Similar experiments were reported by Sundaram et al.<sup>[27]</sup> In short, the **PNCB-co-BP** networks were exposed to a solution containing the protein pepsin at pH 7.4 and pH 3, and the protein adsorption was monitored by SPR kinetics experiments. In addition to these qualitative experiments, the amount of pepsin irreversibly attached to **PNCB-co-BP** after this treatment was quantified by measuring angular reflectivity curves by SPR (Figures 4a and Figure 4b, respectively). The amount of irreversibly adsorbed protein thus determined is given in Table 3. At pH 3, the layer thickness of adsorbed pepsin was as thick as 31.1 nm (Figure 4b). From the data shown in Figure 3b, it can be concluded that the  $\zeta$  potential of the **PNCB-co-BP** network was around 30 mV at this pH due to protonation of its carboxylate groups, that is, the negatively charged pepsin will adhere to the polycationic surface. At a pH of 7.4, the pepsin layer thickness was on average only 0.6 nm thick, and thus reduced by a factor of 50 compared to the amount determined at pH 3 (Table 3 and Figure 4b). This result is also in good agreement with literature, where polyelectrolytic surfaces with low protein adhesion at physiological pH were reported.<sup>[24,28–32]</sup> Interestingly, **PNCB-co-BP** networks have a negative zeta potential at physiological pH. They therefore do not strongly interact with pepsin, which is also negatively charged at low pH.

In a third experiment, pepsin was adsorbed onto the **PNCB-co-BP** network at pH 3, and then the pH of the surrounding buffer was switched to 7.4. The kinetics curve and the full reflectivity scans before exposure to protein and after the pH switch are shown in Figure 4c; the amount of adsorbed pepsin is listed in Table 3. First, the **PNCB-co-BP** network was rinsed with buffer at pH 7.4 to record a baseline (Figure 4c, 0–17 min). Next, it was exposed to buffer with pH 3 (17–33 min). This caused a shift in the reflectivity value, either due to changes in the dielectric properties of the polymer network, or due to increased swelling under these conditions following the protonation of the carboxylate groups of the network. Pepsin was then injected at pH 3 and strongly adsorbed to the surface (33–68 min). Rinsing the surface with buffer at pH 3 could gradually remove some of the adsorbed protein (68–135 min), similarly to the experiment shown in Figure 4b. In contrast, injecting buffer at pH 7.4 (135–150 min) almost immediately reduced the reflectivity back to the same level as the baseline at pH 7.4. As can be seen from the corresponding full reflectivity scans, hardly any pepsin was retained (average layer thickness 0.2 nm), so the networks were able to near-quantitatively release the adsorbed protein. This experiment demonstrates the pH responsiveness of the **PNCB-co-BP** network, and that

this property can be used to switch its properties from protein-adhesive to protein-repellent. AFM height images of the surfaces before and after contact with pepsin (at pH 7.4, pH 3.0, and pH 7.4 → 3.0 → 7.4) are shown in Figure S16, Supporting Information, however except for an increase of surface roughness at pH 3, they do not give any visual evidence about protein adsorption.

## 2.5. Biological Characterization of PNCB-Based Networks

To assess the antimicrobial activity of the different surface-attached **PNCB**-based networks, standardized antimicrobial assays<sup>[17]</sup> have been performed using *Escherichia coli* (*E. coli* ATCC25922) and *Staphylococcus aureus* (*S. aureus* ATCC6538) bacteria. The results of these tests are shown in Figure 5. First, a simplified version of the Japanese Industrial Standard JIS Z 2801 (JIS-Test) with  $5 \times 10^2$  bacteria was used (called screening assay in the following). This assay is used routinely in our lab prior to doing the more elaborate JIS Z 2801 assay in order to screen polymers for general antimicrobial activity. In the screening assay, **PNCB-Homo** was tested against *E. coli* bacteria (Figure 5a). The data shows that no bacteria could be detected after 4 h of incubation, that is, the **PNCB-Homo** networks killed all bacteria as effectively as the positive control, and therefore are antimicrobially active. Due to the limited amount of bacteria used in the screening assay, this information is insufficient to quantify the antimicrobial efficiency of a polymer surface. Therefore, a full JIS-assay with  $10^5$  colony forming units was performed with **PNCB-Homo**, **PNCB-co-BP**, and **PNCB-co-Diazo** (Figure 5). The data shows that **PNCB-Homo** reduces the growth of *E. coli* by about 5 log steps, while **PNCB-co-BP** and **PNCB-co-Diazo** even showed a 6 log reduction and were as effective as the positive control **PZI** (Figure 1, established as highly antimicrobial<sup>[33]</sup> and used in our lab as a control). In addition, **PNCB-co-BP** networks were also effective against *S. aureus* bacteria, with a 4–5 log reduction, and thus a similarly high effectiveness as the positive control (Figure 5d).

For polyelectrolytic networks, this is rather unusual since protein-repellency and antimicrobial activity are typically considered to be mutually exclusive. Recently, our research group reported the first antimicrobial polyelectrolytic network (**PZI**, Figure 1), followed by two more structures with that unusual combination of properties (**PCB** and **IA-PZI**, Figure 1). With **PNCB**, there are now a total of four antimicrobial polyelectrolytics with this property combination known in the literature. The exact origin of the antimicrobial activity is not yet clear. Unfortunately, most polyelectrolytics in the literature are not tested against bacteria. The working hypothesis right now is that acidic metabolites from bacteria protonate the carboxylates of these poly(carboxybetaines). The result is a locally polycationic network in the proximity of the bacteria, which kills them. Without the bacterial metabolites, the carboxylate is deprotonated again and the killed bacteria or their debris can no longer adhere to the surface.<sup>[8]</sup> Clearly, charge switchability alone is not sufficient to explain the antimicrobial activity, or else every poly(carboxybetaine) would be antimicrobially active. The few examples of poly(carboxybetaines) in the literature other than the ones mentioned above, which have been tested for antimicrobial activity were inactive, and thereby show that there is at least one other parameter that needs to be matched to obtain

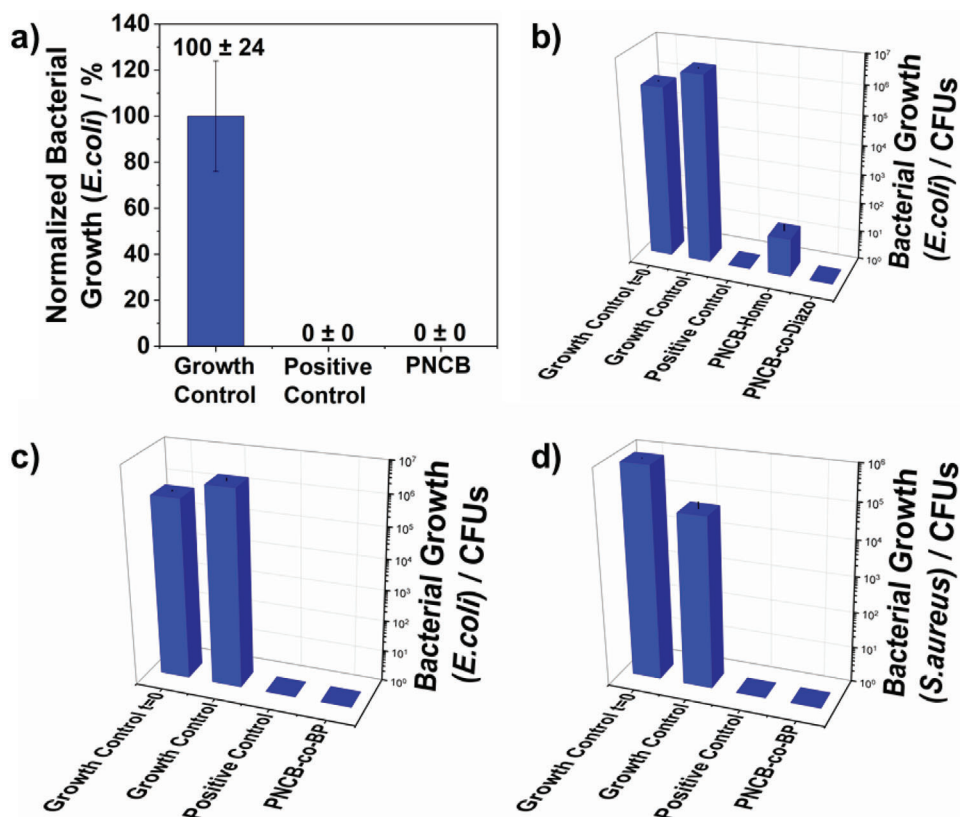


**Figure 5.** Microbiological characterization of different PNCB-based networks. PZI (see Figure 1) was used as positive control in all experiments. a) Normalized growth of *E. coli* on PNCB-Homo in the screening assay; b) growth of *E. coli* on PNCB-Homo and PNCB-co-Diazo in the JIS-assay, c) growth of *E. coli* on PNCB-co-BP in the JIS-assay against, d) growth of *S. aureus* on PNCB-co-BP in the JIS-assay. For the JIS-assays, results from one test replicate are shown. Data from additional replicates are shown in Tables S1–S3, Supporting Information).

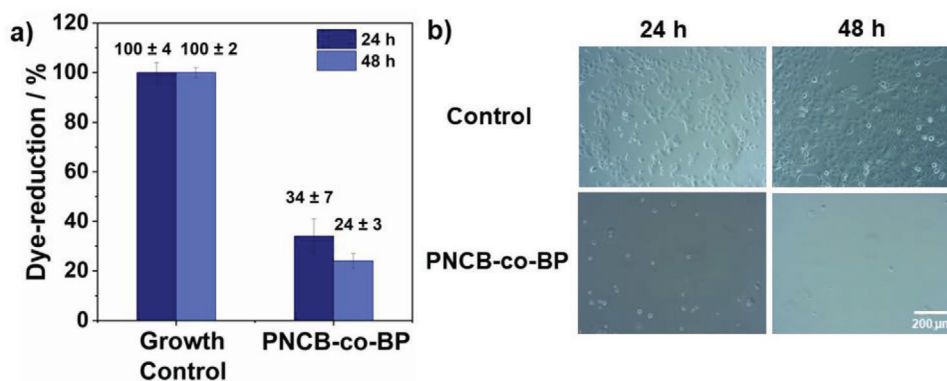


**Figure 6.** Cell biological characterization of PNCB-co-BP networks with HaCaT cells. a) Cell viability after 24 and 48 h incubation time determined by the AlamarBlue assay (shown as dye reduction relative to a growth control (uncoated glass coverslips)); b) optical micrographs of the growth control and the PNCB-co-BP networks after 24 and 48 h incubation time with HaCaT cells.

antimicrobial activity in the protonated state.<sup>[3,5]</sup> Research on antimicrobial polycationic networks suggests that this parameter might be a sufficient amount of hydrophobic groups on the poly(carboxyzwitterions).<sup>[34]</sup>

To assess the toxicity of PNCB-co-BP-coated surfaces, human dermal keratinocytes (HaCaT) have been seeded onto the PNCB-co-BP networks and were incubated for up to 48 h at 37 °C. After

24 and 48 h, the cell metabolism was quantified using the AlamarBlue assay (Figure 6a), and optical micrographs were taken (Figure 6b). As can be seen in Figure 6a, the dye reduction (which is proportional to the cell metabolism) of cells grown on PNCB-co-BP was low compared to the growth control surface (a bare silicon wafer). As can be seen in Figure 6b, the PNCB-co-BP networks are strongly cell repellent, and almost no cells managed

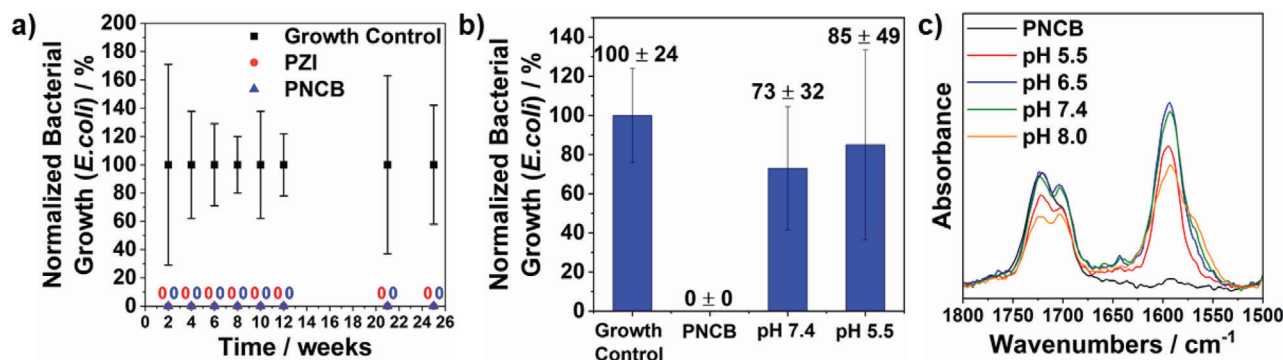


**Figure 7.** Stability of PNCB-co-BP networks: a) Storage stability of PNCB-co-BP networks under ambient conditions. For up to 25 weeks of storage, PNCB-co-BP networks were found to be antimicrobially active against *E. coli* bacteria in the screening assay. b) Application stability. The antimicrobial activity of PNCB-co-BP networks after incubation in different buffers for 24 h at 37 °C was strongly reduced. c) FTIR spectra (C=O double bond region) of PNCB-co-BP networks before and after incubation in aqueous media for 22 days. The ester-band at 1720 cm<sup>-1</sup> decreases during incubation, and a new adsorption band and a shoulder at 1568 cm<sup>-1</sup> appeared, corresponding to carboxylate functionalities.

to adhere to them. Thus, a much smaller number of cells actually metabolized on these materials than on the control surfaces. This result is in good agreement with the literature, where most of the investigated polyelectrolytic surfaces were reported as cell-repellent.<sup>[35]</sup> On these materials, it was also shown with live-dead-staining that the few adhering cells were green, that is, not membrane compromised, and as such was not cell toxic.<sup>[9]</sup> It is commonly assumed that the reason for this behavior is the protein-repellent character of the surfaces, since cell-adhesion is protein-mediated. The only examples of polyelectrolytes to which human cells (in this case, human mucosal keratinocytes) could adhere, as far as we know, are PZI and PSB (Figure 1).<sup>[8]</sup> There is not yet an explanation for these difference in the literature.

## 2.6. Stability of PNCB Networks

The chemical stability of the PNCB-co-BP networks was tested by simulating storage conditions as well as application conditions. For the storage conditions study, the surfaces were kept at ambient conditions (r.t., ambient atmosphere) for several weeks. To simulate conditions of use, the surfaces were stored in aqueous media for a defined time. At the required time points, the materials were removed, and the screening assay (as described in Section 2.5 of this work) was performed.

In the storage conditions study (Figure 7a), no bacteria grew on the PNCB-co-BP networks even after 25 weeks. The same result was observed for PZI networks which were tested as a reference. Concluding, the networks were stable for at least up to 25 weeks. So far, the networks were not tested longer but the study is ongoing.

In the application conditions study, the PNCB-co-BP networks were immersed into different aqueous buffer solutions for 24 h at 37 °C. Afterwards, they were again tested for antimicrobial activity using the screening assay. The results are shown in Figure 7b. It can be seen that the antimicrobial activity is already compromised after one day in aqueous media at different pH values. PZI, IA-PZI, and PCB (Figure 1) showed the same behavior (unpublished data). To find out the reason for this behavior, which was unexpected because PNCB-co-BP did not contain any primary

**Table 4.** Water contact-angle of the PNCB-co-BP networks before and after incubation in buffer.

Contact-angle [°]	Static	Advanced	Receding
Before incubation	22 ± 2	21 ± 1	23 ± 4
After incubation	64 ± 3	58 ± 3	n.d.

**Table 5.** Relative amounts of carbon, nitrogen, and oxygen of the PNCB-co-BP networks before and after incubation in buffer, determined by XPS measurement.

Before incubation			After 24 h in PBS		
C1s	N1s	O1s	C1s	N1s	O1s
73.09%	6.87%	20.04%	76.40%	4.68%	18.92%

amine groups or labile imide rings, the samples were further analyzed by FTIR spectroscopy and XPS. Additionally, water contact-angle measurements were taken see if the hydrophilicity of the network changed after the aqueous treatment (Table 4). Indeed, these data show that the networks became more hydrophobic, indicating that the number of ionic groups has reduced during the exposure to aqueous media. Using the XPS data, the elemental composition of the surfaces before and after the aqueous treatment could be compared (Table 5). The data shows that the relative amounts of nitrogen and oxygen decreased during the aqueous treatment. Since those elements are present in the charged functional groups of the polymer, it can be concluded that the ionic groups in the side chain were eliminated from the polymer during incubation. This result is consistent with the contact angle measurement data.

FTIR measurements of the PNCB-co-BP networks (Figure 6c) showed marked changes in the region where C=O stretching vibrations are found (1500 to 1800 cm<sup>-1</sup>). For a clearer visibility of these changes, the samples were incubated for 22 days at the different pH values. The black curve shows the spectrum of PNCB-co-BP networks before incubation, with three bands in the relevant section of the spectrum: a weak band from the



benzophenone-carbonyl ( $1591\text{ cm}^{-1}$ ), a strong band from the imide present in the benzophenone comonomer ( $1703\text{ cm}^{-1}$ ), and the strong band originating from the ester group of the NCB repeat unit ( $1720\text{ cm}^{-1}$ ). After incubation, the ester band decreased. This is clearly visible in comparison to the imide-band which does not change during the incubation. Notably, the decrease of the ester band is the stronger, the higher the pH of the medium. Additionally, a new strong band at  $1593\text{ cm}^{-1}$  appeared which can be assigned to a carboxylate stretching vibration. This is not surprising, since the carboxylic acid of **PNCB-co-BP** is partially deprotonated in aqueous media. More interestingly, a shoulder ( $1568\text{ cm}^{-1}$ ) appeared at this carboxylate band. This is probably also a carboxylate but in a different chemical surrounding. The increase of this shoulder at increasing pH values is proportional to the decrease of the ester band, which hints at ester hydrolysis.

Summarizing the results from FTIR, XPS, and contact-angle measurements, a loss of charged groups and ester groups has been observed, together with a new carboxylate functionality which developed during the immersion of the **PNCB-co-BP** networks in aqueous media. A suitable conclusion for these results would be a hydrolysis of the ester bond, which cleaves off the side-chain of the polymer. Since the side groups contain the charged moieties of **PNCB-co-BP**, this would explain the higher contact angle and the loss of nitrogen and oxygen in the XPS measurement. The resulting carboxylate would have a different chemical surrounding than the one in the side chain which also explains the carboxylate shoulder in the FTIR spectrum. Another point that supports this hypothesis is the extent of the hydrolysis at different pH values. Ester hydrolysis is faster in basic media than in the acidic range, which would explain the stronger changes of the relevant groups in the FTIR at high pH found in the here presented measurements.

### 3. Conclusion

The aim of this study was to synthesize a pH responsive polyzwitterionic network and demonstrate its switchable protein repellency. With the here presented polyzwitterionic, surface-attached **PNCB**-based networks, such a material could be realized. Physical characterization of these networks showed that they were hydrophilic and that networks with built-in cross-linker (**PNCB-co-BP** and **PNCB-co-Diazo**) were very smooth. **PNCB-Homo** with an additional low molecular mass cross-linker, on the other hand, had a granular morphology. Surface zeta-potential measurements with **PNCB-co-BP** showed that the structure was able to respond to different pH values of the surrounding media. At low pH, the polyzwitterionic groups were protonated, resulting in a polycationic network. It was shown that the adsorption of the protein pepsin on **PNCB-co-BP** was strongly pH dependent. At low pH, the polycationic network adsorbed high amounts of protein, while it repelled most of the protein at physiological pH. Additionally, it could be shown that protein previously adsorbed on the surface (in the polycationic state) could be removed by switching the pH of the medium from pH 3 to pH 7.4. Further, **PNCB**-based networks were antimicrobially active against *E. coli* bacteria, and **PNCB-co-BP** was also active against *S. aureus* (the others were not tested). Thus, the here described **PNCB**-based network had a switchable bioac-

tivity. Unlike in previous publications from our group,<sup>[8,9]</sup> this property was not merely conjectured, but could be demonstrated by the desorption of pepsin when the pH was switched. Thus, the only missing proof for our hypothesis that antimicrobially active polyzwitterions like **PNCB**, **PZI**, **PCB**, and **IA-PZI** are in a polycationic state when exposed to bacteria is to actually demonstrate the polycationic state in situ during biological assays. This, however, is far from trivial, and the object of ongoing studies.

Comparing the properties of **PNCB**-based networks to the previously reported antimicrobial polyzwitterions (Figure 1), one major advantage is the absence of possible intramolecular reactions which limit the stability of the structures. In **PZI** and **IA-PZI**, primary ammonium groups reacted intramolecularly with the ester groups, forming an amide bonds, and thus become inactive against bacteria. The quaternary ammonium groups of **PNCB** (and also of the previously reported **PCB**) do not undergo such reactions. Yet **PCB**, which contains an imide ring which starts to ring-open even at a physiological pH value. **PNCB**-based polymers were designed to carry a hydrolytically more stable ester group. While this group was perfectly stable at room temperature during the physical characterization of **PNCB** materials, unfortunately this work demonstrated that the structure is still not sufficiently stable for long-time exposure to physiological pH and temperature. Thus, to obtain a hydrolytically stable polyzwitterionic structure which can be switched between a polyzwitterionic and a polycationic state, the **PNCB** structure should be further improved by introducing a linker group which is even more stable against hydrolysis. This work is ongoing and will be reported in due course.

### 4. Experimental Section

**Materials:** All materials used, as well as their commercial sources, are listed in Section S1, Supporting Information.

**Instrumentation:** NMR spectra were recorded on a Bruker (Billerica, MA, USA) 250 MHz spectrometer using  $\text{CDCl}_3$ , deuterated methanol ( $\text{CD}_3\text{OD}$ ), or water ( $\text{D}_2\text{O}$ ) as a solvent. GPC, in trifluoroethanol (TFE) with 0.05 M potassium trifluoroacetate (KTFA),  $40\text{ }^\circ\text{C}$ , calibrated with poly(methyl methacrylate) standards) was performed on a PSS PFG Linear M column (PSS, Mainz, Germany) using a Soma UV/Vis detector at a wavelength of 230 nm. Attenuated total reflection Fourier transform infrared spectra (ATR-FTIR) were recorded on a Cary 630 FTIR Spectrometer (Agilent Technologies, Santa Clara, CA, USA). Transmission FTIR spectra were recorded on a Bio-Rad Excalibur spectrometer (Bio-Rad, München, Germany). The polymers were immobilized on double-side polished silicon wafers for the latter experiment using a blank wafer as a background. For the formation of polymeric layers on silicon wafers or glass substrates, a SPIN 150 spin coater (SPS-Europe, Putten, Netherlands) was used with the following parameters: 3000 rpm,  $500\text{ rpm s}^{-1}$ , and 20 s spinning time. For this, the polymer was dissolved in TFE at a concentration of  $30\text{ mg mL}^{-1}$ .

**Physical Characterization:** The thickness of dry polymer layers was measured with a SE400adv ellipsometer (Sentech Instruments GmbH, Berlin, Germany). Three measurements on different spots of the sample were taken, and the average was calculated. AFM was used to analyze the surface topography. A Dimension FastScan from Bruker (Billerica, MA, USA) was used with commercial ScanAsyst Air cantilevers (also from Bruker, length  $115\text{ }\mu\text{m}$ ; width  $25\text{ }\mu\text{m}$ ; spring constant  $0.4\text{ N m}^{-1}$ , resonance frequency  $70\text{ kHz}$ ). All AFM images were recorded in ScanAsyst Air-mode. The obtained images were analyzed and processed with the Nanoscope Analysis 9.1 software. XPS was measured on a PerkinElmer PHI 5600 ESCA system (PerkinElmer, Waltham, MA, USA). The X-ray source was a Mg anode



with an energy of 1253.6 eV. The samples were measured at room temperature with an angle of 45°. Zeta-potential was measured via electrokinetic surface characterization which was performed on an electrokinetic analyzer with an integrated titration unit (SurPass, AntonPaar GmbH, Graz, Austria). The analyzer was equipped with an adjustable gap cell. Ag/AgCl electrodes were used to detect the streaming current. The polymer was spin-cast on fused silica substrates (20 × 10 × 1 mm, MaTeck, Jülich, Germany) and put into the measuring cell. Before each measurement, the electrolyte hoses were rinsed with ultrapure water until a conductivity of <0.06 mS m<sup>-1</sup> was reached. The measuring cell was mounted and the electrolyte solution (1 mM KCl) was prepared. The pH of the electrolyte solution was adjusted to pH 2.5 or pH 10 with 0.1 M HCl or 0.1 M NaOH respectively prior to filling the electrolyte hoses. The gap height was adjusted to ≈105 μm while the system was rinsed for 3 min at 300 mbar. Titration measurement was performed with 0.05 M NaOH or 0.05 M HCl. The target pressure of the pressure ramp was set to 400 mbar. After titration and before each measurement cycle, the system was rinsed for 3 min at 300 mbar. The pressure program was as follows: target pressure, 400 mbar; maximum time, 20 s; current measurement; two repetitions. A representative titration curve (ζ-potential versus pH) is shown in Figure 3. The isoelectric point (IEP, pH where the zeta potential was zero) was determined from the curve. The pK has been estimated graphically from the titration curve as reported previously.<sup>[9]</sup>

**Protein Adsorption:** Protein adsorption was studied using SPR spectroscopy. To set up the experiment, an angular scan of the coated substrate under a flow of buffer was performed to detect the plasmon signal minimum. The protein adsorption experiments in the kinetic mode were then carried out at  $\Theta_{\text{exp}} = \Theta_{\text{min}} - 1$  by monitoring signal intensity at that angle versus time. First, the baseline intensity at that angle against buffer was recorded. The protein solution was then injected (pepsin solution at a concentration of 1 mg mL<sup>-1</sup> in triethanolamine buffer (pH 7.4) or citrate buffer (pH 3.0), flow rate 50 μL h<sup>-1</sup>). After reaching an equilibrium, buffer was injected to remove any loosely adhering protein. The difference of the reflectivity value before protein injection and after the final buffer wash gives a qualitative estimate to whether the surface is protein adhesive. To quantitatively determine the thickness of the adsorbed protein layer after the kinetics experiment, the surfaces were rinsed with distilled water for 15 min to remove residual salt and dried under nitrogen flow. Afterwards, another angular reflectivity curve was measured. The thickness of each layer of the material was calculated by simulations of the reflectivity curves based on the Fresnel equations as described previously.<sup>[8]</sup>

**Antimicrobial Activity:** To test the antimicrobial activity of the polymer networks, modifications of the Japanese Industrial Standard JIS Z 2801 were used as published elsewhere.<sup>[17]</sup> For antimicrobial activity screening, *E. coli* (*E. coli* ATCC25922) was used. Approximately 5 × 10<sup>2</sup> bacteria were incubated for 4 h on 1 × 1 cm<sup>2</sup> test samples and controls (five replicates each). They were detached using 0.9% NaCl solution with Tween80. 250 μL of that suspension was spread on tryptic soy agar plates and incubated at 37 °C and 5% CO<sub>2</sub> for 18 to 24 h. The colony-forming units (CFUs) were counted after incubation and reported as percent growth relative to the growth control. The antimicrobial activity of polymer networks that were found to be highly active in the screening assay was confirmed using a modified JIS Assay with 10<sup>6</sup> CFUs with either *E. coli* or *S. aureus* (*S. aureus* ATCC6538). Key changes in this assay compared to the original protocol of the Japanese Industrial Standard JIS Z 2801 were the reduction of the sample size to 2.5 × 2.5 cm<sup>2</sup>, and a corresponding volume of the bacterial suspension to 100 μL (containing ≈1 × 10<sup>6</sup> CFUs). The CFUs were determined after 0 and 24 ± 1 h, and were reported as log reduction relative to the negative control.

**Cell Viability:** Human dermal keratinocytes, HaCaT (CLS, Eppelheim, Germany) were used to test the cell compatibility. Cells were cultured in Dulbecco's Modified Eagle's Medium (DMEM) supplemented with 4.5 g L<sup>-1</sup> glucose, 2 mM L-glutamine, and 10% Fetal Calf Serum (FCS). At a cell confluence of 80–90%, the cells were detached with TrypLETM express (life technologies, Darmstadt, Germany). 1 × 10<sup>5</sup> cells were seeded on round glass coverslips (15 mm in diameter; thickness No. 2; ORSatec, Bobingen, Germany) and incubated in FCS-free DMEM at 37 °C/5% CO<sub>2</sub> to allow the cells to settle. After 4 h, 50% of the medium was discarded

and replaced of DMEM with double FCS concentration, yielding a normal FCS concentration for further cultivation (24 and 48 h).

The AlamarBlue assay was performed and analyzed according to the manufacturer's protocol (Biorad, Feldkirchen, Germany). For this, 500 μL growth medium was removed and replaced with fresh 500 μL DMEM with FCS containing 10% AlamarBlue solution. Cells were incubated under physiological conditions for at least 2 h. Supernatant was centrifuged at 300 g for 5 min, and the fluorescence intensity was measured (excitation at 540 nm; measurement at 590 nm) using the microplate reader Infinite F Nano Plus (Tecan, Crailsheim, Germany). Within one experiment, triplicates were generated for all samples and controls. The experiment was repeated twice. Optical images were obtained using a Primovert Microscope (Zeiss, Oberkochen, Germany) and processed using the related ZEN blue software (Zeiss, Oberkochen, Germany).

**Synthesis:** 2-(Dimethylamino)ethyl-bicyclo[2.2.1]hept-5-ene-2-carboxylate (**2**): Compound **2** was synthesized according to a literature procedure. Bicyclo[2.2.1]hept-5-ene-2-carboxylic acid (2.00 g, 14.4 mmol, 1.0 equiv.), dimethylaminoethanol (1.60 mL, 1.42 mg, 15.92 mmol, 1.1 equiv.), and triphenylphosphane (4.18 g, 15.92 mmol, 1.1 equiv.) were dissolved in tetrahydrofuran (anhydrous, 10 mL). The solution was cooled in an ice-bath and diisopropyl-diazene-1,2-dicarboxylate (DIAD) (3.12 mL, 3.02 g, 1.1 equiv.) was added dropwise. The reaction mixture was stirred at room temperature overnight. Afterwards, the solvent was removed under reduced pressure and citric acid solution (aq., 1 M, 5 mL) was added to the residue. After stirring for 30 min, the precipitate was filtered off and washed. The filtrate was washed with ethyl acetate (3 × 15 mL). K<sub>2</sub>CO<sub>3</sub> was added to the aqueous phase until its pH was >8, followed by extraction with Et<sub>2</sub>O:n-hexane (9:1, 10 × 10 mL). The combined organic phases were dried over Na<sub>2</sub>SO<sub>4</sub> and the solvents were removed under reduced pressure.

<sup>1</sup>H-NMR (250 MHz, CDCl<sub>3</sub>): δ = 1.33–1.60 (m, 3H, CH–CH<sub>2</sub>, CH–CH<sub>b</sub>), 1.94 (dt, 1H, CH–CH<sub>a</sub>, J<sub>1</sub> = 11.9 Hz, J<sub>2</sub> = 3.9 Hz), 2.26–2.35 (m, 1H, CO–CH), 2.32 (s, 6H, CH<sub>3</sub>), 2.60 (t, 2H, N–CH<sub>2</sub>, <sup>3</sup>J<sub>6,5</sub> = 5.8 Hz), 2.91–2.97 (m, 1H, CO–CH–CH), 3.04–3.09 (m, 1H, CH<sub>2</sub>–CH), 4.22 (t, 2H, O–CH<sub>2</sub>, <sup>3</sup>J<sub>5,6</sub> = 5.8 Hz), 6.10–6.17 (m, 2H, CH=CH) ppm.

<sup>13</sup>C-NMR (250 MHz, CDCl<sub>3</sub>): δ = 30.27 (CH–CH<sub>2</sub>), 41.51 (CH<sub>2</sub>–CH), 42.92 ((C=O)–CH), 45.61 (CH<sub>3</sub>), 46.17 ((C=O)–CH–CH), 46.54 (bridgehead-CH<sub>2</sub>), 57.78 (N–CH<sub>2</sub>), 62.13 (O–CH<sub>2</sub>), 135.63 (CH=CH–CH–CH<sub>2</sub>), 137.91 (CH=CH–CH–CH<sub>2</sub>), 176.06 (C=O) ppm.

m/z = 210.15 g mol<sup>-1</sup>

2-((Bicyclo[2.2.1]hept-5-ene-2-carbonyl)oxy)-N-(2-carboxyethyl)-N,N-dimethylethan-1-ammonium chloride (**NCB**): Compound **2** (400.0 mg, 1.92 mmol, 1.0 equiv.) was dissolved in THF (anhydrous, 2 mL). β-Propiolactone (0.14 mL, 165.7 mg, 2.3 mmol, 1.2 equiv.) was added and the mixture was stirred at room temperature for 4 h. The precipitate was filtered, washed with THF and n-hexane and dried. In a second step, the product was dissolved in a HCl-solution (in dioxane, 4 M, 2 mL) and stirred at room temperature for 30 min. The solvent was removed under reduced pressure and the residue was dried.

<sup>1</sup>H-NMR (250 MHz, D<sub>2</sub>O): δ = 1.25–1.42 (m, 3H, CH–CH<sub>2</sub>, CH–CH<sub>b</sub>), 1.75 (dt, 1H, CH–CH<sub>a</sub>, J<sub>1</sub> = 11.7 Hz, J<sub>2</sub> = 4.0 Hz), 2.26 (dd, 1H, CO–CH), 2.64 (t, 2H, CO–CH<sub>2</sub>, <sup>3</sup>J<sub>9,8</sub> = 12.0 Hz), 2.82–2.91 (m, 1H, CO–CH–CH), 2.95–3.01 (m, 1H, CH<sub>2</sub>–CH), 3.09 (s, 6H, CH<sub>3</sub>), 3.56 (t, 2H, CO–CH<sub>2</sub>–CH<sub>2</sub>, <sup>3</sup>J<sub>8,9</sub> = 12.0 Hz), 3.65–3.68 (m, 2H, N–CH<sub>2</sub>), 4.43–4.54 (m, 2H, O–CH<sub>2</sub>), 6.05–6.16 (m, 2H, CH–CH) ppm.

<sup>13</sup>C-NMR (250 MHz, CDCl<sub>3</sub>): δ = 28.21 (CH–CH<sub>2</sub>), 30.43 (bridgehead-CH<sub>2</sub>), 41.82 (CH<sub>2</sub>–CH), 43.27 ((C=O)–CH–CH), 46.43 (CH<sub>3</sub>), 52.04 (CH<sub>2</sub>–N–CH<sub>2</sub>), 58.64 (O–CH<sub>2</sub>), 60.46 ((C=O)–CH<sub>2</sub>), 62.88 ((C=O)–CH), 136.01 (CH=CH–CH–CH<sub>2</sub>), 138.86 (CH=CH–CH–CH<sub>2</sub>), 173.38 (CH<sub>2</sub>–(C=O)), 178.08 (CH–(C=O)) ppm.

m/z = 282.17 g mol<sup>-1</sup>

**Synthesis of PNCB Homopolymers (PNCB-Homo):** NCB monomer (200 mg, 0.63 mmol, 95 equiv.) was dissolved in TFE (dried, distilled, and degassed). In a separate flask, the Grubbs 3<sup>rd</sup> Gen catalyst (4.8 mg, 0.0066 mmol, 1.0 equiv.) was dissolved in DCM (dried and distilled). The catalyst-solution was added to the monomer solution in one shot with an overall ratio TFE:DCM of 1:1 (v/v). After stirring the mixture for 1 h at room-temperature, ethyl vinyl ether (0.5 mL) was added to stop the

reaction. The mixture was stirred at room-temperature for another 30 min and the solvents were removed under reduced pressure. Finally, the crude was redissolved in TFE and precipitated from Et<sub>2</sub>O.

<sup>1</sup>H-NMR (250 MHz, D<sub>2</sub>O):  $\delta$  = 1.05–1.27 (m, 1H, CH–CH–CH<sub>b</sub>), 1.61–2.08 (m, 3H, CH–CH–CH<sub>a</sub>, CH–CH<sub>2</sub>), 2.49–2.75 (m, 2H, CO–CH<sub>2</sub>), 2.80–3.01 (m, 3H, CH–CH<sub>2</sub>–CH–CH), 3.09 (s, 6H, CH<sub>3</sub>), 3.54–3.77 (m, 4H, CH<sub>3</sub>–N–CH<sub>3</sub>), 4.37–4.56 (m, 2H, O–CH<sub>2</sub>), 5.15–5.55 (m, 2H, CH=CH) ppm.

**Synthesis of PNCB Copolymer PNCB-co-BP:** NCB monomer (200 mg, 0.63 mmol, 83 equiv.) was dissolved in TFE (dried, distilled, and degassed). In a second flask, the benzophenone-carrying monomer **3** (26.6 mg, 0.07 mmol, 9 equiv.) was dissolved in dichloromethane (dried and distilled) and the solution was added to the NCB monomer solution. In a separate flask, the Grubbs 3<sup>rd</sup> Gen catalyst (5.5 mg, 0.008 mmol, 1.0 equiv.) was dissolved in DCM (dried and distilled). The catalyst solution was added to the monomer solution in one shot with an overall ratio TFE:DCM of 1:1 (v/v). After stirring the mixture for 1 h at room-temperature, ethyl vinyl ether (1 mL) was added to stop the reaction. The mixture was stirred at room-temperature for another 30 min and the solvents were removed under reduced pressure. Finally, the crude was redissolved in TFE and precipitated from Et<sub>2</sub>O.

<sup>1</sup>H-NMR (250 MHz, D<sub>2</sub>O):  $\delta$  = 1.05–1.27 (m, 1H, CH–CH–CH<sub>b</sub>), 1.61–2.08 (m, 3H, CH–CH–CH<sub>a</sub>, CH–CH<sub>2</sub>), 2.49–2.75 (m, 2H, CO–CH<sub>2</sub>), 2.80–3.01 (m, 3H, CH–CH<sub>2</sub>–CH–CH), 3.09 (s, 6H, CH<sub>3</sub>), 3.54–3.77 (m, 4H, CH<sub>3</sub>–N–CH<sub>3</sub>), 4.37–4.56 (m, 2H, O–CH<sub>2</sub>), 5.15–5.55 (m, 2H, CH=CH) ppm.

**Synthesis of PNCB Copolymer PNCB-co-Diazo:** NCB monomer (200 mg, 0.63 mmol, 94 equiv.) was dissolved in TFE (dried, distilled, and degassed). In a second flask, the diazo-ester carrying monomer **4** (22.4 mg, 0.07 mmol, 10 equiv.) was dissolved in dichloromethane (dried and distilled) and the solution was added to the NCB monomer solution. Separately, the Grubbs 3<sup>rd</sup> Gen catalyst (4.8 mg, 0.007 mmol, 1.0 equiv.) was dissolved in DCM (dried and distilled). The catalyst solution was added to the monomer solution in one shot with an overall ratio TFE:DCM of 1:1 (v/v). After stirring the mixture for 1 h at room-temperature, ethyl vinyl ether (1 mL) was added to stop the reaction. The mixture was stirred at room-temperature for another 30 min and the solvents were removed under reduced pressure. Finally, the crude was redissolved in TFE and precipitated from Et<sub>2</sub>O.

<sup>1</sup>H-NMR (250 MHz, D<sub>2</sub>O):  $\delta$  = 1.05–1.27 (m, 1H, CH–CH–CH<sub>b</sub>), 1.61–2.08 (m, 3H, CH–CH–CH<sub>a</sub>, CH–CH<sub>2</sub>), 2.49–2.75 (m, 2H, CO–CH<sub>2</sub>), 2.80–3.01 (m, 3H, CH–CH<sub>2</sub>–CH–CH), 3.09 (s, 6H, CH<sub>3</sub>), 3.54–3.77 (m, 4H, CH<sub>3</sub>–N–CH<sub>3</sub>), 4.37–4.56 (m, 2H, O–CH<sub>2</sub>), 5.15–5.55 (m, 2H, CH=CH) ppm.

## Supporting Information

Supporting Information is available from the Wiley Online Library or from the author.

## Acknowledgements

Funding of this work from the Bundesministerium für Bildung und Forschung (German Ministry for Education and Research, BMBF) in the VIP+ technology transfer program under the grant acronym ANTIBUG is gratefully acknowledged. Thanks to Vera Bleicher for help with the microbiological experiments.

Open access funding enabled and organized by Projekt DEAL.

## Conflict of Interest

The authors declare no conflict of interest.

## Data Availability Statement

Research data are not shared.

## Keywords

antimicrobial polymers, polyelectrolytes, polyzwitterions, protein-repellent polymers, stimulus-responsive polymers

Received: January 21, 2021

Revised: April 20, 2021

Published online: May 24, 2021

- [1] WHO, Report on Global Surveillance of Antimicrobial Resistance.
- [2] J. O'Neill, The review on antimicrobial resistance – tackling drug-resistant infections globally: Final report and recommendations, [https://amr-review.org/sites/default/files/160518\\_Final%20paper\\_with%20cover.pdf](https://amr-review.org/sites/default/files/160518_Final%20paper_with%20cover.pdf) (accessed: May 8, 2018).
- [3] G. Cheng, H. Xue, Z. Zhang, S. Chen, S. Jiang, *Angew. Chem., Int. Ed.* **2008**, *47*, 8831.
- [4] L. Mi, S. Jiang, *Angew. Chem., Int. Ed.* **2014**, *53*, 1746.
- [5] Z. Cao, L. Mi, J. Mendiola, J.-R. Ella-Menye, L. Zhang, H. Xue, S. Jiang, *Angew. Chem., Int. Ed.* **2012**, *51*, 2602.
- [6] W. Hartleb, J. S. Saar, P. Zou, K. Lienkamp, *Macromol. Chem. Phys.* **2016**, *217*, 225.
- [7] P. Zou, W. Hartleb, K. Lienkamp, *J. Mater. Chem. A* **2012**, *22*, 19579.
- [8] M. Kurowska, A. Eickenscheidt, D.-L. Guevara-Solarte, V. T. Widyaya, F. Marx, A. Al-Ahmad, K. Lienkamp, *Biomacromolecules* **2017**, *18*, 1373.
- [9] M. Kurowska, A. Eickenscheidt, A. Al-Ahmad, K. Lienkamp, *ACS Appl. Bio Mater.* **2018**, *1*, 613.
- [10] A. Jain, L. S. Duvvuri, S. Farah, N. Beyth, A. J. Domb, W. Khan, *Adv. Healthcare Mater.* **2014**, *3*, 1969.
- [11] K. Lienkamp, A. E. Madkour, G. N. Tew, *Adv. Polym. Sci.* **2013**, *251*, 141.
- [12] E.-R. Kenawy, S. D. Worley, R. Broughton, *Biomacromolecules* **2007**, *8*, 1359.
- [13] F. Siedenbiedel, J. C. Tiller, *Polymers* **2012**, *4*, 46.
- [14] A. Laschewsky, *Polymers* **2014**, *6*, 1544.
- [15] A. Laschewsky, *Curr. Opin. Colloid Interface Sci.* **2012**, *17*, 56.
- [16] E. Wischerhoff, N. Badi, A. Laschewsky, J.-F. Lutz, *Adv. Polym. Sci.* **2011**, *240*, 1.
- [17] A. Schneider-Chaabane, V. Bleicher, S. Rau, A. Al-Ahmad, K. Lienkamp, *ACS Appl. Mater. Interfaces* **2020**, *12*, 21242.
- [18] S. Colak, G. N. Tew, *Langmuir* **2012**, *28*, 666.
- [19] E. Riga, J. Saar, R. Erath, M. Hechenbichler, K. Lienkamp, *Polymers* **2017**, *9*, 686.
- [20] D. A. Rankin, S. J. P'Pool, H.-J. Schanz, A. B. Lowe, *J. Polym. Sci., Part A: Polym. Chem.* **2007**, *45*, 2113.
- [21] G. Becker, Z. Deng, M. Zober, M. Wagner, K. Lienkamp, F. R. Wurm, *Polym. Chem.* **2018**, *9*, 315.
- [22] O. Prucker, T. Brandstetter, J. Rühle, *Biointerphases* **2018**, *13*, 010801.
- [23] O. Prucker, T. Brandstetter, J. Rühle, *Biointerphases* **2017**, *13*, 010801.
- [24] J. Koc, E. Schönemann, A. Amuthalingam, J. Clarke, J. A. Finlay, A. S. Clare, A. Laschewsky, A. Rosenhahn, *Langmuir* **2019**, *35*, 1552.
- [25] M. Kurowska, V. Widyaya, A. Al-Ahmad, K. Lienkamp, *Materials* **2018**, *11*, 1411.
- [26] S. Colak, G. N. Tew, *Langmuir* **2012**, *28*, 666.
- [27] H. S. Sundaram, J.-R. Ella-Menye, N. D. Brault, Q. Shao, S. Jiang, *Chem. Sci.* **2014**, *5*, 200.
- [28] S. Jiang, Z. Cao, *Adv. Mater.* **2010**, *22*, 920.
- [29] J. Ladd, Z. Zhang, S. Chen, J. C. Hower, S. Jiang, *Biomacromolecules* **2008**, *9*, 1357.
- [30] C.-J. Lee, H. Wu, Q. Tang, B. Cao, H. Wang, H. Cong, J. Zhe, F. Xu, G. Cheng, *Langmuir* **2015**, *31*, 9965.
- [31] B. Li, P. Jain, J. Ma, J. K. Smith, Z. Yuan, H.-C. Hung, Y. He, X. Lin, K. Wu, J. Pfaendtner, S. Jiang, *Sci. Adv.* **2019**, *5*, eaaw9562.



- [32] W. Yang, H. Xue, W. Li, J. Zhang, S. Jiang, *Langmuir* **2009**, *25*, 11911.
- [33] M. Kurowska, A. Eickenscheidt, D. L. Guevara-Solarte, V. T. Widyaya, F. Marx, A. Al-Ahmad, K. Lienkamp, *Biomacromolecules* **2017**, *18*, 1373.
- [34] P. Zou, D. Laird, E. K. Riga, Z. Deng, F. Dorner, H.-R. Perez-Hernandez, D. L. Guevara-Solarte, T. Steinberg, A. Al-Ahmad, K. Lienkamp, *J. Mater. Chem. B* **2015**, *3*, 6224.
- [35] S. Paschke, K. Lienkamp, *ACS Appl. Polym. Mater.* **2020**, *2*, 129.